Title: **Biogenic iron preserves structures during fossilization: A hypothesis**

Subtitle: Iron from decaying tissues may stabilize their morphology in the fossil record

Farid Saleh[1], Allison C. Daley[2], Bertrand Lefebvre[1], Bernard Pittet[1], and Jean Philippe Perrillat[1]

[1]Université de Lyon, Université Claude Bernard Lyon1, École Normale Supérieure de Lyon, CNRS, UMR5276, LGL-TPE, Villeurbanne, France
[2]Institute of Earth Sciences, University of Lausanne, Géopolis, CH-1015 Lausanne, Switzerland

Corresponding author: Farid Saleh
Email: farid.saleh@univ-lyon1.fr

Summary

In this study, we hypothesize that iron from labile biological tissues, liberated during decay, may have played a role in inhibiting loss of anatomical information during fossilization of extinct organisms. Most tissues in the animal kingdom contain iron in different forms. The most widely distributed iron-bearing molecule in modern taxa is ferritin, a globular protein that contains iron crystallites in the form of ferrihydrite minerals. Iron concentrations in ferritin are particularly high and ferrihydrites are extremely reactive. When organisms are decaying on the sea floor under anoxic environmental conditions, ferrihydrites may initialize the selective pyritization (replication in FeS_2) of some tissues. This model explains why some decay-prone tissues are preserved, while other more resistant structures decayed and are absent in many fossils. It also implies that structures described as brains in Cambrian arthropods are not fossilization artifacts but instead a source of information on the anatomical evolution at the dawn of complex animal life.

Keywords: exceptional fossil preservation, nervous systems, Burgess Shale, Fezouata Shale, Chengjiang Biota, taphonomy, mineralization

1. Introduction

Inspecting the fossil record is crucial to understanding the biology of past life on earth. Exceptionally preserved biotas, preserving soft-bodied metazoans (e.g. sponges; early chordates) and their labile anatomies (e.g. digestive tracts, muscles, and nervous systems) constitute a unique window on ancient ecosystems[1–3]. For instance, the Burgess Shale deposit in Canada yielded a considerable number of fossils shedding lights on spectacular Cambrian taxa preserved in high fidelity[4–10]. Exceptionally preserved soft parts in fossils from the Fezouata Shale (Ordovician, Morocco) were decisive in ending long-standing debates on the systematic affinities of various enigmatic taxa (e.g. machaeridians, stylophorans)[11–13]. The Chengjiang Biota (Cambrian, China) has also yielded a considerable amount of soft arthropod taxa with complex nervous systems[14–16]. In most cases, nervous tissues from the Chengjiang Biota are pyritized (i.e. preserved in FeS_2) or show the association of pyrite and organic matter[14–17]. Pyritized tissues are frequently preserved alone in the fossils, while other tissues or organs (except the cuticle or body walls) are completely absent[17]. Experimental taphonomic studies investigating how biological tissues decay under various, controlled laboratory conditions questioned the validity of these paleontological discoveries by showing that nervous systems have little to no chance of preservation because they are observed to be rapidly lost under experimental conditions[18–20]. These experimental results have consequently given rise to contrasting conceptual frameworks in the paleontology and evolutionary biology communities[21–23]. Although vital to constrain preservation[23], experimental decay data should be interpreted carefully and not projected directly onto enigmatic features in the geological record because fossils are not simply rotten carcasses and decay resistance is an imperfect indicator of fossilization potential[24]. Currently, there is no model accounting for the preservation of a specific labile tissue in a specimen where other more resistant tissues are completely absent. We investigate preservation patterns in such problematic structures and compare it to the patterns of pyritization in non-altered sediments, and propose an explanation for the contrast observed between the fossil record and modern decay experiments.

2. Enigmatic structures are preserved in pyrite and organic matter

Anatomical structures described as brains in fossils from the Chengjiang Biota were investigated using X-ray fluorescence mapping, which revealed the presence of carbon and iron[17] (Fig. 1a-d). Electron microscopy shows that iron occurs either as small euhedral crystals (around 2 microns in size) or as framboids (around 10 microns in size)[17] (Fig. 1e-h). Pyrite crystal morphology indicates that pyritization occurred very early during the fossilization process, shortly after the death of the organism[25,26]. Carbon in these fossils is preserved as compressed dark films[17] (Fig. 1i, j). Chengjiang fossils broken through the middle show pyrite overlaying carbonaceous films on both parts[17], pointing to a centrifugal pattern of pyritization (Fig. 1k). Centrifugal pyritization, similar to patterns of tissue preservation in the Chengjiang Biota, is also present in fresh core sediments (Fig. 2a) from levels with exceptional preservation within the Fezouata Shale, where Raman spectroscopy identified large pyrite clusters surrounded by organic matter (Fig. 2b-d).

FeS_2 precipitation in sediments requires decaying organic material, and iron that is usually provided by surrounding sediments in addition to sulfates SO_4^- from sea waters [27,28]. Under sulfate-reducing conditions, bacteria transform organic matter and sulfates into HS^- and then to hydrogen sulfides H_2S, which react with Fe in a series of reactions to form pyrite [26–28]. If the sediment surrounding dead animals is poor in organic matter, as was the case in the Fezouata Shale[29], sulfate reduction is limited to decaying carcasses[29]. Within a decaying carcass, anatomical features can react differently to decay[30]. Easily degradable structures (e.g. tissues and organs formed of cells)[3] constitute a hotspot for H_2S production, whereas

more resistant structures (e.g. biomineralized parts), do not produce enough H_2S, and thus do not pyritize[31]. Furthermore, decay discrepancies exist even between different fast decaying cellular structures. Some cellular structures are solely degraded by external bacterial communities, while others degrade under the activity of their internal microbial biota and enzymes as well[30,32]. If decay by external bacteria is dominant and iron is available, pyritization starts at the outer part of the organic material where both H_2S and Fe are present, leading to a centripetal pattern of preservation (Fig. 3a). This pattern is observed in the fossil record[27] and does not refute occurrences of centrifugal pyritization, because some tissues decay under the activity of their internal bacteria and enzymes. If such internal decay is dominant and iron is present, more H_2S is produced internally, leading to the centrifugal pattern of preservation (Fig. 3b). It is likely that preserved structures in the Chengjiang Biota and the Fezouata Shale decayed under the activity of their internal microbial biotas and enzymes in the presence of iron. The proposed model based on H_2S limitation and production patterns[25,27,31] can explain (1) the centrifugal pyritization of nervous systems in Cambrian arthropods and (2) the association of this anatomy to non-pyritized cuticular body walls that did not produce enough H_2S for their pyritization[25,31]. However, it fails to explain the selective pyritization of a specific cellular structure (i.e. nervous system) while other internal structures (e.g. digestive and vascular systems) decayed, producing H_2S, but did not pyritize. Thus, it is crucial to investigate patterns of iron distribution in the sediment surrounding decaying carcasses.

3. Abiotic iron is not fast enough to preserve labile tissues

The most classical and widely accepted sources of iron for pyritization are abiotic[28,33]. In the Fezouata Shale, iron oxides found in sediments (e.g. hematite α-Fe_2O_3; Fig. 2b-d) constitute only a small fraction of the rock (i.e. <1%)[26]. However, in a comparable way to numerous Cambrian sites with exceptional fossil preservation, iron-rich silicates such as berthierine/chamosite are dominant (i.e. between 5 and 15% of the total rock composition)[26,34]. Berthierine/chamosite results from the transformation of a primary clay mineral (e.g. glauconite, odinite, kaolinite, or other similar precursor minerals)[35] under anoxic conditions and high iron concentrations[26]. Thus, iron in this mineralogical phase gives an estimate of the quantity of iron in the environment[26,34,35]. The formation of berthierine/chamosite in the Fezouata Shale required at least ~ 8.10^{-5} M (defined here the M notation) of iron (see supplementary material). These concentrations are high and are slightly less than the ones in modern anoxic sediments at 10^{-4}M and are enough to pyritize at the site of decay[27]. Thus, in theory and in terms of concentrations, abiotic iron is not a limiting parameter in levels with exceptional preservation in the Fezouata Shale[26] in a similar way to sites with exceptional fossil preservation from the Cambrian[34,36]. However, there must have been other parameters controlling the availability of this iron during soft tissues degradation and inhibiting pyrite from replicating all internal systems. Laboratory experiments have shown that most anatomical structures in soft animals decay very fast within hours or days after death[18,20,37]. For instance, nervous tissues decayed under 11 days for chordates and under 4 days for ecdysozoans[18,20]. On the contrary, most iron-rich phases in contact with H_2S require longer times to deliver their iron (Table 1)[38]. This timing exceeds the timing of biological tissue decay, especially for labile anatomies such as the brain [18,20,32,37]. Thus, another source of available iron must exist in order to selectively pyritize a tissue/organ shortly after the death of the organism.

4. Biogenic iron is available during decay

If abiotic iron is not enough to start the pyritization process investigation on biogenic iron source should take place. In analyzed samples (i.e. thin sections) from the Fezouata Shale,

maghemite (i.e. γ-Fe_2O_3 structurally similar to magnetite) is associated with pyrite (Fig. 2b-d). Two widely recognized mechanisms for maghemite formation exist[39,40]. In the first mechanism, lepidocrocite, a fibrous iron oxide-hydroxide, transforms partially to maghemite at temperatures around 200°C and completely at temperatures higher than 570°C[39]. Maghemite can also result from buried ferrihydrites at temperatures between 100 and 300° C[40]. Sediments from the Fezouata Shale were cooked at temperatures between 100 and 200°C[26,41]. These temperatures and the absence of lepidocrocite in the analyzed samples but also from tens of other intervals in the Fezouata Shale[26] indicate that maghemite in these samples originates most probably from ferrihydrites. Ferrihydrite is a mineral with a wide biological distribution that can explain why maghemite is only found in association with pyritized organic matter and not in the sediment.

In all animals, ferritin is a metalloprotein that stores an excess of iron in the form of a hydrous ferric oxide-phosphate mineral $[FeO(OH)]_8$ $[FeO(H_2PO_4)]$ similar in structure to the mineral ferrihydrite[42,43]. Ferritin-ferrihydrites are found in nervous systems, muscles and sensory organs such as the eyes[44–46]. Ferritin is capable of storing as many as 4,500 iron atoms in its core (i.e. concentration equivalent to 0.25M)[46]. Increased accumulations of ferritin-ferrihydrites were evidenced in marine invertebrates after their exposure to dysoxic/anoxic conditions[47] comparable to the environments in which animals from the Chengjiang Biota and the Fezouata Shale were preserved[48,49]. In experimental studies, it was shown that under bacterial sulfate reducing (BSR) conditions and when sulfates are present, ferrihydrites release high quantities (~ 87%) of reactive Fe[50] (i.e. 0.22M). This iron delivery is 40% higher than the yield from the same quantity of hematite[50]. Furthermore, ferrihydrite is the fastest to deliver reactive iron (Table 1), with a half-life under BSR conditions of only 2.8 hours[38]. Ferrihydrite is also a solid phase meaning that it does not migrate[51]. Thus, 0.11M of iron becomes available *in-situ* within a couple of hours of the start of decay. These concentrations are well above those in modern anoxic sediments[27], and are definitely enough to initiate pyritization at the site of decay.

5. Biogenic iron explains the selective pyritization of soft anatomies

Ferrihydrite in biological tissues constitutes a local source that rapidly provides high quantities of reactive Fe[38] that can initialize the process of pyritization. In this sense, shortly after the death of an organism, decay of the most labile tissue starts producing H_2S. If this tissue contains ferrihydrites, it produces as well a considerable amount of reactive iron (Fig. 4). The produced H_2S and Fe react to form pyrite nuclei (Fig. 4) that further growth from H_2S and Fe availability as decay occurs (Fig. 4). The extensive activity of decay leads also to the degradation of more resistant tissues (Fig. 4). However, if these less labile tissues are iron poor, they produce only H_2S without iron (Fig. 4). Thus, the replication of such tissue in pyrite is not initiated, leading to a loss of the original morphology or even the complete disappearance of the tissue/organ (Fig. 4). When abiotic iron becomes available, it can play a role in pyrite growth in tissues that previously provided biogenic iron (Fig. 4). This hypothesis shows how biogenic iron stabilizes the morphology of decay-prone anatomical structures, before the less reactive iron phases become available.

6. Hypothesis testing requires a multidisciplinary approach

Although fossil mineralization is common in the geological record[53–58], little work has been done to investigate the role of tissue chemistry during the mineralization process. Recently, it was suggested that the recurrent association of a particular mineralogical phase

fluorapatite, Fe-sulfides (pyrite, pyrrhotite)

with a specific tissue in La Voulte-sur-Rhône (Jurassic, France), (precise the nature of the mineralogical phase ? the type of tissue? And/or organism? Age and context sedim) can be due to differences in the original biochemical signal of the organic matter[52].
crustacean fossils preserved within carbonate-rich concretions from the Jurassic Konservat-Lagerstätte of La Voulte-sur-Rhône (Ardèche, France)
However, much work remains to be done to precise the fate and behavior of biogenic iron during the taphonomic processes, and fully enlighten the black box of pyritization.

In order to test the hypothesis and determine the precise roles played by biogenic iron and iron from sediments, several lines of investigation should be undertaken combining geochemical, biological and experimental taphonomy approaches.

It would be ideal to start testing the hypothesis on nonweathered fossils. However, to our knowledge, no pyritized fossils from completely fresh sediments are discovered yet. Until then, yielding investigations on fresh pyrite, not particularly associated with any fossil can also be helpful because pyrite formation requires organic matter, and different organic materials reflect different original biochemical compositions.
>> these sentences are not clear for me…

Iron isotopic investigations on pyrite crystals from both the sediments and the pyritized fossils would help to decipher the multiple iron-sources and their role in pyritization. If these isotopic investigations were made at the nanoscale, they can inform on the source and chronology of iron delivery from the initiation of pyrite precipitation to the subsequent pyrite crystals growth.

What about sulfur isotopes?
Do you think minor elements (bio-related?) would be of interest?

Biological approaches are also very helpful in testing this biogenic iron hypothesis, for example by making a comparison between iron concentrations in different modern animal groups and those measured in pyritized tissues found in the fossil record. An even more detailed approach would be to quantify iron in different kinds of tissues within the same group. For instance, according to this hypothesis, if a specific group shows a higher concentration of iron in a specific tissue, we would expect to find this particular structure pyritized more often than the others in the geological record.
All these quantitative data will also help calibrate the new proposed model and understand its feasibility in natural environments. Most importantly, future decay experiments should focus not only on the general environmental conditions that lead to exceptional preservation, but also on the chemical signature surrounding each tissue during its degradation independently from the physical ability of this tissue to resist decay. These decay experiments should be done in the presence of different sediment compositions and under different bacterial communities to see if decaying carcasses act variously under different environmental conditions. Once iron sources, iron quantities in biological tissues, decay behavior, in addition to favorable sedimentological phases are discovered, pyrite precipitation from biological tissues could be replicated in laboratory aquariums.

Further isotopic investigations along this lines of the data presented here should be undertaken on pyrite crystals should to determine iron sources at different stages of the mineralization process. Additionally, the possible role of a biogenic iron source in other exceptionally preserved biotas could be explored in this context[40]. For example, at the Burgess Shale (Cambrian, Canada), nervous systems are preserved as carbonaceous compressions without any pyrite[41,42] since overall conditions were favorable for phosphatization[43]. Nevertheless, berthierine, an iron-rich mineral known to slow down decay[44], is found in all levels with exceptional preservation. Future studies should investigate if this iron-rich mineral, also reported in hundreds of other intervals with exceptional preservation around the world[26], is preferentially associated to specific labile soft parts.
Biological approaches for hypothesis testing including quantitative iron-analysis of modern tissues and animals using mass spectrometry to help calibrate the new proposed model.
Finally, future decay experiments should focus not only on the general environmental conditions that lead to exceptional preservation, but also on the chemical signature surrounding each tissue during its degradation independently from the physical ability of this tissue to resist decay.

7. Conclusions and outlook

The present biogenic iron hypothesis helps us understand the sole presence of the most-labile tissues in some specimens where other more decay-resistant soft parts are absent. It also shows that pyritization starts very early during decay, preserving in high fidelity tissues that are originally iron-rich, resolving the morphological accuracy of Cambrian arthropod brains. Furthermore, it indicates that both decay experiments and paleontological descriptions are complementary, not incompatible. It opens new avenues of research by highlighting the importance of tissue chemistry during the fossilization process especially in the case of nervous tissues that are preserved in carbonaceous compressions without any pyrite [59–61].

Acknowledgments

Figure 1a-j is used with minor edits from Ma et al., Preservational pathways of corresponding brains of a Cambrian euarthropod, Current Biology, Volume 25, Issue 22, p. 7, 2015, with permission from Elsevier. This paper is a contribution to the TelluS-INTERRVIE project ‘Géochimie d'un *Lagerstätte* de l'Ordovicien inférieur du Maroc’ (2019) funded by the INSU (Institut National des Sciences de l'Univers, France), CNRS. This paper is also a contribution to the International Geoscience Program (IGCP) Project 653 – The onset of the Great Ordovician Biodiversification Event. The Raman facility in Lyon (France) is supported by the INSU. ACD’s contribution is supported by Grant no. 205321_179084 from the Swiss National Science Foundation. The authors thank Gilles Montagnac for assistance during Raman spectroscopy analyses. We also thank Robert Raiswell, Christian Klug, and the anonymous reviewers for their comments and remarks.

Conflict of interest

None

References

[1] P. Van Roy, P. J. Orr, J. P. Botting, L. A. Muir, J. Vinther, B. Lefebvre, K. El Hariri, D. E. G. Briggs, *Nature* **2010**, *465*, 215.

[2] A. C. Daley, J. B. Antcliffe, H. B. Drage, S. Pates, *Proc. Natl. Acad. Sci.* **2018**, *115*, 5323.
[3] F. Saleh, J. B. Antcliffe, B. Lefebvre, B. Pittet, L. Laibl, F. Perez Peris, L. Lustri, P. Gueriau, A. C. Daley, *Earth Planet. Sci. Lett.* **2020**, *529*, DOI 10.1016/j.epsl.2019.115873.
[4] J. Moysiuk, M. R. Smith, J.-B. Caron, *Nature* **2017**, *541*, 394.
[5] J. Moysiuk, J. B. Caron, *Proc. R. Soc. B Biol. Sci.* **2019**, *286*, 20182314.
[6] K. Nanglu, J. B. Caron, *Curr. Biol.* **2018**, *28*, 319.
[7] A. C. Daley, G. E. Budd, J. B. Caron, G. D. Edgecombe, D. Collins, *Science (80-.).* **2009**, *323*, 1597.
[8] J. Vannier, J. Liu, R. Lerosey-Aubril, J. Vinther, A. C. Daley, *Nat. Commun.* **2014**, *5*, 1.
[9] M. R. Smith, J.-B. Caron, *Nature* **2010**, *465*, 469.
[10] T. P. Topper, L. C. Strotz, L. E. Holmer, Z. Zhang, N. N. Tait, J. B. Caron, *BMC Evol. Biol.* **2015**, *15*, 42.
[11] J. Vinther, P. Van Roy, D. E. G. Briggs, *Nature* **2008**, *451*, 185.
[12] J. Vinther, L. Parry, D. E. G. Briggs, P. Van Roy, *Nature* **2017**, *542*, 471.
[13] B. Lefebvre, T. E. Guensburg, E. L. O. Martin, R. Mooi, E. Nardin, M. Nohejlová, F. Saleh, K. Kouraïss, K. El Hariri, B. David, *Geobios* **2019**, *52*, DOI 10.1016/j.geobios.2018.11.001.
[14] G. Tanaka, X. Hou, X. Ma, G. D. Edgecombe, N. J. Strausfeld, *Nature* **2013**, *502*, 364.
[15] P. Cong, X. Ma, X. Hou, G. D. Edgecombe, N. J. Strausfeld, *Nature* **2014**, *513*, 538.
[16] X. Ma, X. Hou, G. D. Edgecombe, N. J. Strausfeld, *Nature* **2012**, *490*, 258.
[17] X. Ma, G. D. Edgecombe, X. Hou, T. Goral, N. J. Strausfeld, *Curr. Biol.* **2015**, *25*, 2969.
[18] R. S. Sansom, S. E. Gabbott, M. A. Purnell, *Nature* **2010**, *463*, 797.
[19] D. J. E. Murdock, S. E. Gabbott, G. Mayer, M. A. Purnell, *BMC Evol. Biol.* **2014**, *14*, DOI 10.1186/s12862-014-0222-z.
[20] R. S. Sansom, *Sci. Rep.* **2016**, *6*, 1.
[21] J. Liu, M. Steiner, J. A. Dunlop, D. Shu, *Proc. R. Soc. B Biol. Sci.* **2018**, *285*, DOI 10.1098/rspb.2018.0051.
[22] F. Saleh, B. Lefebvre, A. W. Hunter, M. Nohejlová, *Micros. Today* **2020**, *28*, 2.
[23] M. A. Purnell, P. J. C. Donoghue, S. E. Gabbott, M. E. McNamara, D. J. E. Murdock, R. S. Sansom, *Palaeontology* **2018**, *61*, 317.
[24] L. A. Parry, F. Smithwick, K. K. Nordén, E. T. Saitta, J. Lozano-Fernandez, A. R. Tanner, J.-B. Caron, G. D. Edgecombe, D. E. G. Briggs, J. Vinther, *BioEssays* **2018**, *40*, 1700167.
[25] S. E. Gabbott, H. Xian-guang, M. J. Norry, D. J. Siveter, *Geology* **2004**, *32*, 901.
[26] F. Saleh, B. Pittet, J. Perrillat, B. Lefebvre, *Geology* **2019**, *47*, 1.
[27] J. D. Schiffbauer, S. Xiao, Y. Cai, A. F. Wallace, H. Hua, J. Hunter, H. Xu, Y. Peng, A. J. Kaufman, *Nat. Commun.* **2014**, *5*, 5754.
[28] R. Raiswell, K. Whaler, S. Dean, M. . Coleman, D. E. . Briggs, *Mar. Geol.* **1993**, *113*, 89.
[29] R. R. Gaines, D. E. G. Briggs, P. J. Orr, P. Van Roy, *Palaios* **2012**, *27*, 317.
[30] D. E. G. Briggs, A. J. Kear, *Paleobiology* **1993**, *19*, 107.
[31] Ú. C. Farrell, *Paleontol. Soc. Pap.* **2014**, *20*, 35.
[32] A. D. Butler, J. A. Cunningham, G. E. Budd, P. C. J. Donoghue, *Proc. R. Soc. B Biol. Sci.* **2015**, *282*, 20150476.
[33] R. Raiswell, D. E. Canfield, R. A. Berner, *Chem. Geol.* **1994**, *111*, 101.
[34] R. P. Anderson, N. J. Tosca, R. R. Gaines, N. Mongiardino Koch, D. E. G. Briggs,

Geology **2018**, *46*, 347.
[35] D. Tang, X. Shi, G. Jiang, X. Zhou, Q. Shi, *Am. Mineral.* **2017**, *102*, 2317.
[36] E. A. Sperling, C. J. Wolock, A. S. Morgan, B. C. Gill, M. Kunzmann, G. P. Halverson, F. A. Macdonald, A. H. Knoll, D. T. Johnston, *Nature* **2015**, *523*, 451.
[37] A. D. Hancy, J. B. Antcliffe, *Geobiology* **2020**.
[38] D. E. Canfield, R. Raiswell, S. Bottrell, *Am. J. Sci.* **1992**, *292*, 659.
[39] T. S. Gendler, V. P. Shcherbakov, M. J. Dekkers, A. K. Gapeev, S. K. Gribov, E. McClelland, *Geophys. J. Int.* **2005**, *160*, 815.
[40] L. Mazzetti, P. J. Thistlethwaite, *J. Raman Spectrosc.* **2002**, *33*, 104.
[41] G. M. H. Ruiz, U. Helg, F. Negro, T. Adatte, M. Burkhard, *Swiss J. Geosci.* **2008**, *101*, 387.
[42] F. M. Michel, V. Barron, J. Torrent, M. P. Morales, C. J. Serna, J.-F. Boily, Q. Liu, A. Ambrosini, A. C. Cismasu, G. E. Brown, *Proc. Natl. Acad. Sci.* **2010**, *107*, 2787.
[43] N. D. Chasteen, P. M. Harrison, *J. Struct. Biol.* **1999**, *126*, 182.
[44] K. Hoda, C. L. Bowlus, T. W. Chu, J. R. Gruen, *Emery Rimoin's Princ. Pract. Med. Genet.* **2013**, 1.
[45] E. M. Aldred, C. Buck, K. Vall, E. M. Aldred, C. Buck, K. Vall, *Pharmacology* **2009**, 331.
[46] D. Dunaief, A. Cwanger, J. L. Dunaief, *Handb. Nutr. Diet Eye* **2014**, 619.
[47] K. Larade, K. B. Storey, *J. Exp. Biol.* **2004**, *207*, 1353.
[48] F. Saleh, Y. Candela, D. A. T. Harper, M. Polechovà, B. Pittet, B. Lefebvre, *Palaios* **2018**, *33*, 535.
[49] E. L. O. Martin, B. Pittet, J.-C. Gutiérrez-Marco, J. Vannier, K. El Hariri, R. Lerosey-Aubril, M. Masrour, H. Nowak, T. Servais, T. R. A. Vandenbroucke, P. Van Roy, R. Vaucher, B. Lefebvre, *Gondwana Res.* **2016**, *34*, 274.
[50] Y.-L. Li, H. Vali, J. Yang, T. J. Phelps, C. L. Zhang, *Geomicrobiol. J.* **2006**, *23*, 103.
[51] S. Wang, L. Lei, D. Zhang, G. Zhang, R. Cao, X. Wang, J. Lin, Y. Jia, *J. Hazard. Mater.* **2020**, *384*, 121365.
[52] C. Jauvion, S. Bernard, P. Gueriau, C. Mocuta, S. Pont, K. Benzerara, S. and Charbonnier, *Palaeontology* **2019**, 1.
[53] D. E. Briggs, S. H. Bottrell, R. and Raiswell, *Geology* **1991**, *19(12)*, 1221.
[54] T. A. Hegna, M. J. Martin, S. A. Darroch, *Geology* **2017**, *45*, 199.
[55] L. Frey, A. Pohle, M. Rücklin, C. Klug, *Lethaia* **2019**.
[56] J. Rust, A. Bergmann, C. Bartels, B. Schoenemann, S. Sedlmeier, G. Kühl, *Arthropod Struct. Dev.* **2016**, *45*, 140.
[57] T. W. Kammer, C. Bartels, W. I. Ausich, *Lethaia* **2016**, *49*, 301.
[58] R. Raiswell, R. Newton, S. H. Bottrell, P. M. Coburn, D. E. Briggs, D. P. Bond, S. W. Poulton, *Am. J. Sci.* **2008**, *308*, 105.
[59] J. Ortega-Hernández, R. Lerosey-Aubril, S. Pates, *Proc. R. Soc. B Biol. Sci.* **2019**, *286*, 20192370.
[60] J. Ortega-Hernández, *Curr. Biol.* **2015**, *25*, 1625.
[61] L. Parry, J.-B. Caron, *Sci. Adv.* **2019**, *5*, eaax5858.
[62] S. Das, M. J. Hendry, *Chem. Geol.* **2011**, *290*, 101.

Figure captions

Figure 1. Preservation of Cambrian brains in *Fuxanhuia protensa* from the Chengjiang Biota. a) YKLP 15006 shows dark brown areas interpreted as nervous tissues under direct illumination. b) Carbon distribution in the studied specimen. c) Iron distribution. d) Merged iron and carbon signals show an almost perfect superposition between these two elements. White arrows indicate the rare places were both elements do not co-occur. e-h) Iron is

preserved in small euhedral and framboidal pyrite. i, j) Minerals overlay dark compressed carbonaceous material. The distribution of carbonaceous films under pyrite minerals in both part and counter-part suggest a centrifugal pattern of pyritization (k).

Figure 2. Pyritization in the Fezouata Shale. Pyrite crystals marked by white arrows in fresh core deposits (a) showing a centrifugal pattern of pyritization (b, c). Colored points in (b) and (c) correspond to the spectra shown in (d). Iron oxide phase identification is based on Raman peak indexation in natural samples[62].

Label each peak with the value of the Raman shift in cm-1, it is easier for the reader to compare data.

For the hematite and maghemite, do you have signal in the 1000- 1600 cm-1 range for comparaison with the other spectra??

Figure 3. Patterns of soft tissue decay. a) Soft parts decaying under the activity of external bacteria lead to a centripetal pyritization. b) Soft parts decaying under their own bacterial community and enzymes contribute in a centrifugal pyritization.

Figure 4. Hypothesis for labile tissue preservation and resistant tissue loss.

Iron phase	Half-life
Goethite	11.5 days
Hematite	31 days
Magnetite	105 years
Reactive silicates	230 years
Sheet silicates	84000 years
Augite, amphibole	>84000 years

401 Table 1. Half-lives of iron phases under permissive conditions for pyrite precipitation.
402 (references ?) – what do you mean for "reactive" silicates?

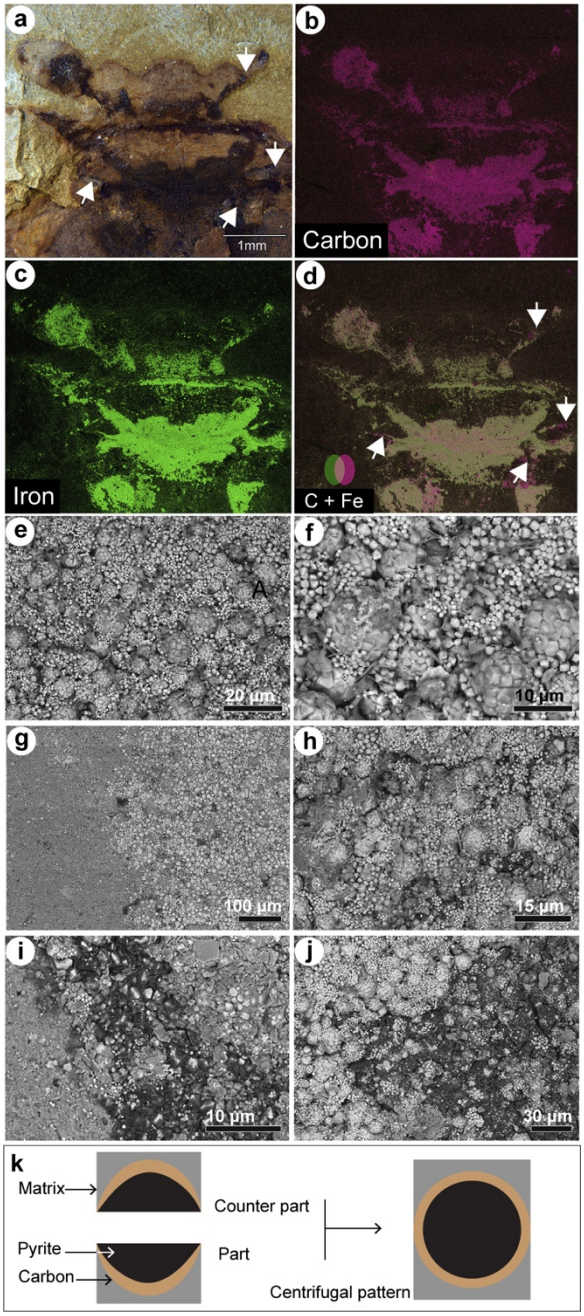
a
1mm
b
Carbon
c
Iron
d
C + Fe
e
A
20 μm
f
10 μm
g
100 μm
h
15 μm
i
10 μm
j
30 μm
k
Matrix
Pyrite
Carbon
Counter part
Part
Centrifugal pattern

Figure 1

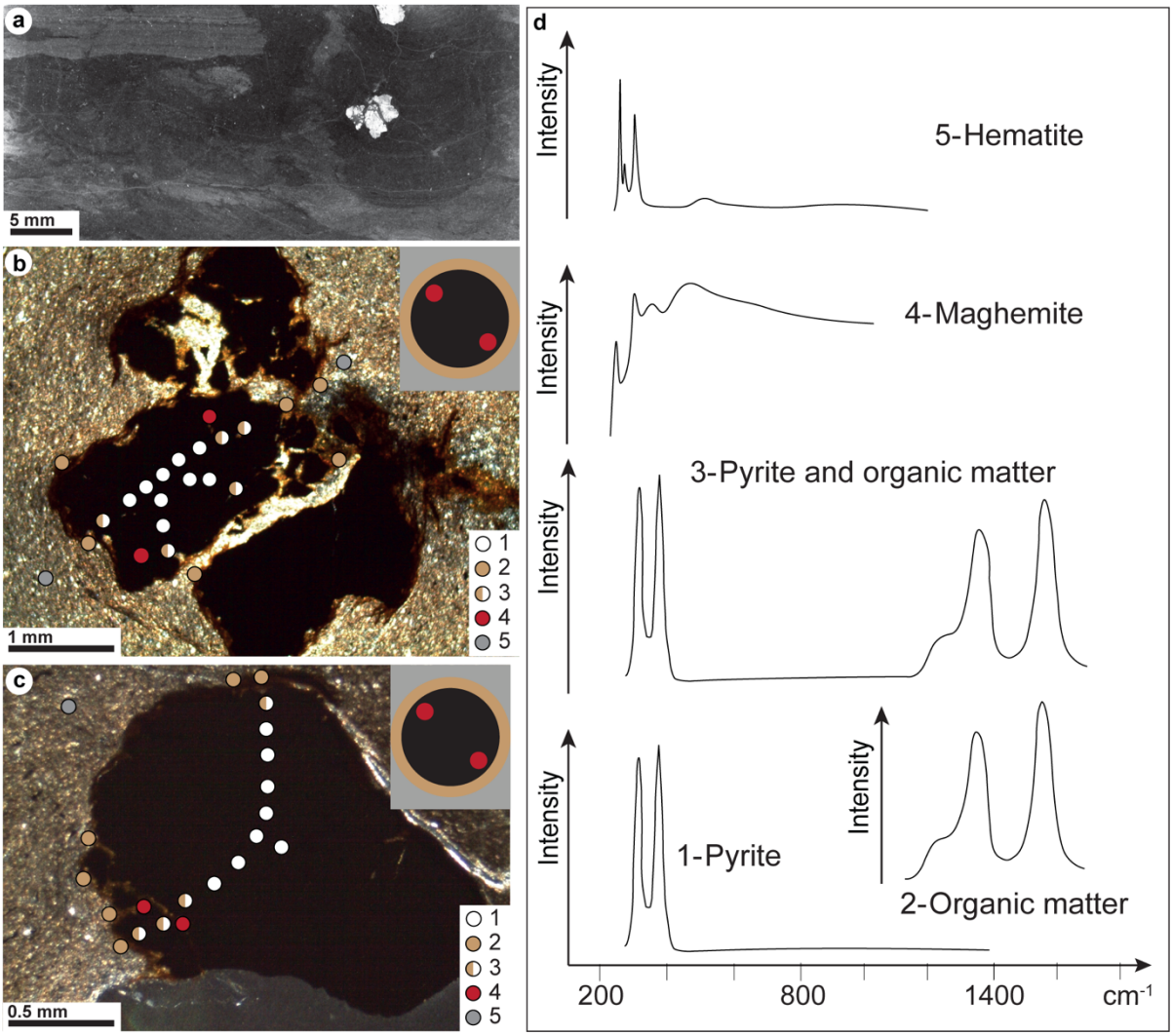
a
5 mm
b
1 mm
1
2
3
4
5
c
0.5 mm
1
2
3
4
5
d
Intensity
5-Hematite
Intensity
4-Maghemite
Intensity
3-Pyrite and organic matter
Intensity
1-Pyrite
Intensity
2-Organic matter
200
800
1400
cm-1

Figure 2

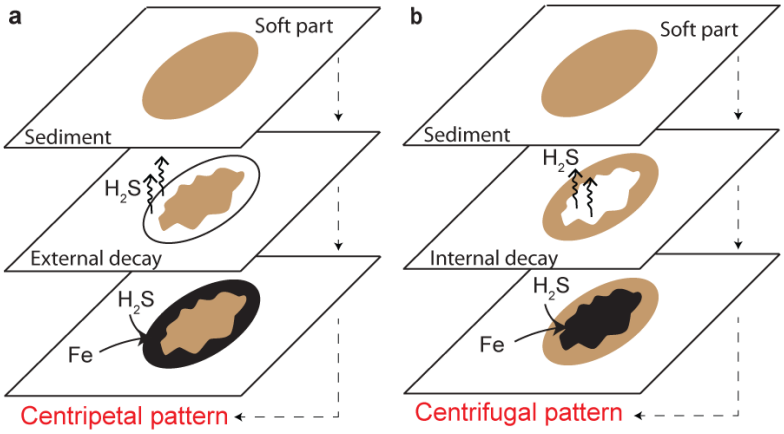

Figure 3

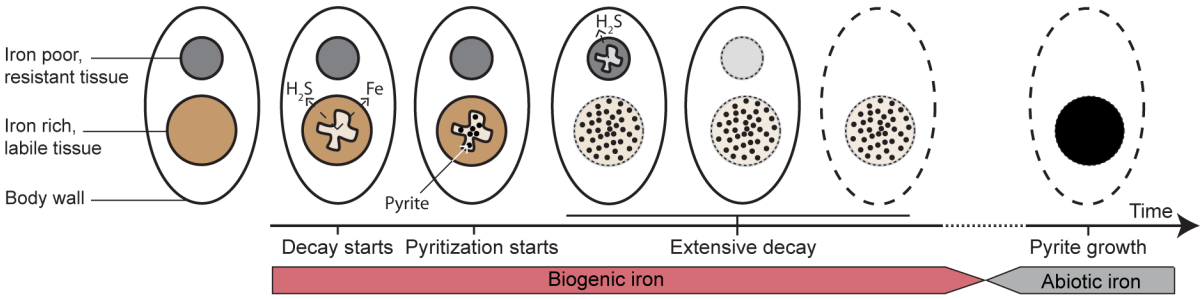

Figure 4